NSR 4-1

JPL CONTRACT NO. 954219

(NASA-CR-149234) PULSED THERMIONIC CONVERTER STUDY Final Report (Rasor Associates, Inc., Sunnyvale, Calif.) 38 p HC A03/MF A01 CSCL 21C

N77-12123

Unclas G3/20 56388

INDUCTIVELY COUPLED THERMIONIC MAGNETOPLASMADYNAMIC SPACECRAFT ELECTRIC PROPULSION

FINAL REPORT

BY EDWARD J. BRITT

APRIL 1976

RASOR ASSOCIATES INCORPORATED
420 PERSIAN DRIVE
SUNNYVALE, CALIFORNIA 94086

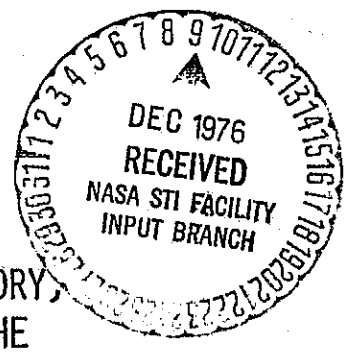

THIS WORK PERFORMED FOR THE JET PROPULSION LABORATORY, CALIFORNIA INSTITUTE OF TECHNOLOGY, SPONSORED BY THE NATIONAL AERONAUTICS AND SPACE ADMINISTRATION CONTRACT NAS7-100

NSR 4-1

JPL CONTRACT NO. 954219

INDUCTIVELY COUPLED THERMIONIC MAGNETOPLASMADYNAMIC SPACECRAFT ELECTRIC PROPULSION

FINAL REPORT

BY EDWARD J. BRITT

APRIL 1976

RASOR ASSOCIATES INCORPORATED
420 PERSIAN DRIVE
SUNNYVALE, CALIFORNIA 94086

THIS WORK PERFORMED FOR THE JET PROPULSION LABORATORY, CALIFORNIA INSTITUTE OF TECHNOLOGY, SPONSORED BY THE NATIONAL AERONAUTICS AND SPACE ADMINISTRATION CONTRACT NAS7-100

ACKNOWLEDGEMENT

This work was performed for the Jet Propulsion Laboratory. The encouragement and guidance of the project by E. V. Pawlik is gratefully acknowledged.

Cooperative interaction with the School of Engineering and Applied Science at Princeton University is also acknowledged. Significant contributions to the technical work have been made by Mr. Kenn E. Clark, Research Engineer, and Prof. Robert G. Jahn, Dean of the School of Engineering at Princeton.

ABSTRACT

A nuclear electric propulsion concept using a thermionic reactor inductively coupled to a magnetoplasmadynamic accelerator (MPD arc jet) is described and the results of preliminary analyses are presented. In this system, the MPD thruster operates intermittently at higher voltages and power levels than the thermionic generating unit. A typical thrust pulse from the MPD arc jet in this study is characterized by power levels of 1 to 4 MWe, a duration of 1 msec, and a duty cycle of ~20%. The thermionic generating unit operates continuously but with a lower power level ~0.4 MWe. Energy storage between thrust pulses is provided by building up a large current in an inductor using the output of the thermionic converter array. Periodically, the charging current is interrupted and the energy stored in the magnetic field of the inductor is utilized for a short duration thrust pulse. The results of the preliminary analysis show that a coupling effectiveness of approximately 85 to 90% is feasible for a nominal 400 KWe system with an inductive unit suitable for a flight vehicle. Optimized values of the total specific mass of the system including the thermionic reactor, the inductor, and the MPD thruster are estimated in the range of 23 to 24 kg/KWe.

TABLE OF CONTENTS

1.0 NOMENCLATURE

Roman Letters

B_s : Parameter used in calculating the inductance of a long solenoid

d : Mean diameter of the inductor, cm

F : Parameter used in calculating the inductance of a long solenoid

I : Current, amps or kiloamps (kA)

$\hat{I}$: Maximum value of the current in a cycle, amps or kiloamps (kA)

$\tilde{I}$: Minimum value of the current in a cycle, amps or kiloamps (kA)

I_o : Short circuit current of thermionic converter array, amps

L : Inductance of the solenoid inductor, μh

h : Length of the inductor, cm

M_L : Mass of the inductor, kg

N : Number of turns in the inductor

P : Net power supplied to thruster, KWe

P_o : Maximum electric power available from the thermionic reactor, KWe

R : Resistance of the inductor winding, ohms

R_p : Total resistance of the current buildup part of the circuit, ohms

R_s : Resistance of the MPD thruster part of the circuit, ohms

s : Thickness of the inductor winding, cm

T : Time between pulses for current buildup, msec

t* : Duration of the thrust pulse, msec

V_c : Voltage of the thermionic converter array, volts

V_F : Parameter in the approximate thruster V-I curve, 30 volts

V_o : Open circuit voltage of the thermionic converter array, volts

V_T : Voltage of the MPD thruster, volts

Greek Leters:

α_M : Specific mass of the MPD thruster, kg/KWe

α_S : Specific mass of the complete system, kg/KWe

α_R : Specific mass of the thermionic reactor, kg/KWe

α_T : Specific mass of the switching transistors, kg/KWe

α_{TR} : Specific mass of the transistor radiator, kg/KWe

β : Parameter in the approximate thruster V-I curve, 1.2×10^{-6} $(amp)^{-2}$

η : Coupling effectiveness, %

τ : Time constant for current buildup, msec

ρ : Temperature dependent resistivity, $\mu\Omega$-cm

θ : Temperature of the inductor, ^{o}K

2.0 INTRODUCTION

Providing propulsion power for deep space missions is often best accomplished with a nuclear electric system. An attractive choice for the power system is a nuclear reactor which uses thermionic conversion for electrical generation. The thermionic reactor is a compact, simple system with no moving parts and a high heat rejection temperature which permits a smaller radiator to be used for dissipating the waste heat. Other advantages for spacecraft power include reliability (no single point failures), long life, and a low specific mass (Ref. 1).

The characteristics of the thruster unit must be optimized for each mission. The thrust variables which must be considered include efficiency of conversion, specific impulse, power level, and specific mass. The MPD thruster has many advantages for spacecraft electric propulsion. A principal advantage of MPD devices over ion rockets is the high thrust density available with the arc jet (typically 1 to 10 N/cm^2). This high thrust density usually allows a significant savings in the mass of the system.

However, efficient operation of the MPD thruster is achieved at power levels (in the megawatt range) which are higher than optimum for many missions. Furthermore, the output of the thermionic converter array is low voltage DC which requires voltage transformation to match the requirements of the MPD arc jet. The differences in power levels between the thruster and the thermionic generating unit combined with the need for power conditioning have led to a system design in which power is transferred to the thruster by means of inductive energy storage.

The thruster is operated in quasi-steady or pulse mode while the thermionic generating unit operates continuously. Between pulses, energy is stored in the magnetic field of a large inductor and dissipated in each short duration thrust pulse. The operating cycle begins with a relatively long charging period (several msec). During this time the current is built up in the windings of the inductor. The charging current is interrupted at the end of the charging period. Next follows the short thrust period ($\sim$ 1 msec) where the current decays rapidly to a lower value. The rapidly changing magnetic flux in the inductor generates a high voltage to power the thruster. The only other required power conditioning element is the switching device(s) to interrupt the charging current.

3.0 SYSTEM DESCRIPTION

3.1 Vehicle Configuration

The thermionic reactor design and spacecraft configuration which form a basis of this work have been developed by previous studies at Jet Propulsion Laboratory (Refs. 1 & 2). The design chosen for the spacecraft is an end thrust type of vehicle which is shown in Fig. 1. The thermionic reactor is located at the rear of the spacecraft behind the radiation shield. The inductor must be configured to fit inside the 23° shadow cone of the radiation shield.

3.2 Thermionic Reactor

Design of the thermionic reactor has been carried out primarily by personnel at Los Alamos Scientific Laboratory as a subcontract to JPL (Refs. 2 & 3). The reactor system is an out-of-core design which uses high temperature heat pipes to transfer heat from a fast spectrum compact reactor to an array of thermionic converters. The configuration of the reactor system (Ref. 2) is shown in Fig. 2. Electrical connections between converters are made in a direction transverse to the axis of the heat pipes. The output bus bars are arranged in 6 layers which are accessible for connections at the periphery of the thermionic converter array.

The emitter temperature of the thermionic converters is $\sim 1650^{\circ}K$ and the collector temperature is $\sim 900^{\circ}K$. Average power density is approximately 6 watts/cm^2. The area of each converter is a 162.6 cm^2. There are 540 converters in the complete power package (Ref. 2).

Various combinations of series-parallel connections for the thermionic converter array can produce output voltages from $\sim$ 3 volts to $\sim$ 54 volts with correspondingly different currents. The optimum voltage for the inductive coupled MPD thruster depends upon resistive and switching losses as well as the variation of thruster performance with current. Determination of the optimum connection arrangement is not possible because detailed data on the variation of thruster efficiency with operating current are not available. Compromise values of the reactor current and voltage were selected for this study which produce currents of $\sim$ 12,000 amps at $\sim$ 39 volts. The total power at the bus bars is 474 Kwe.

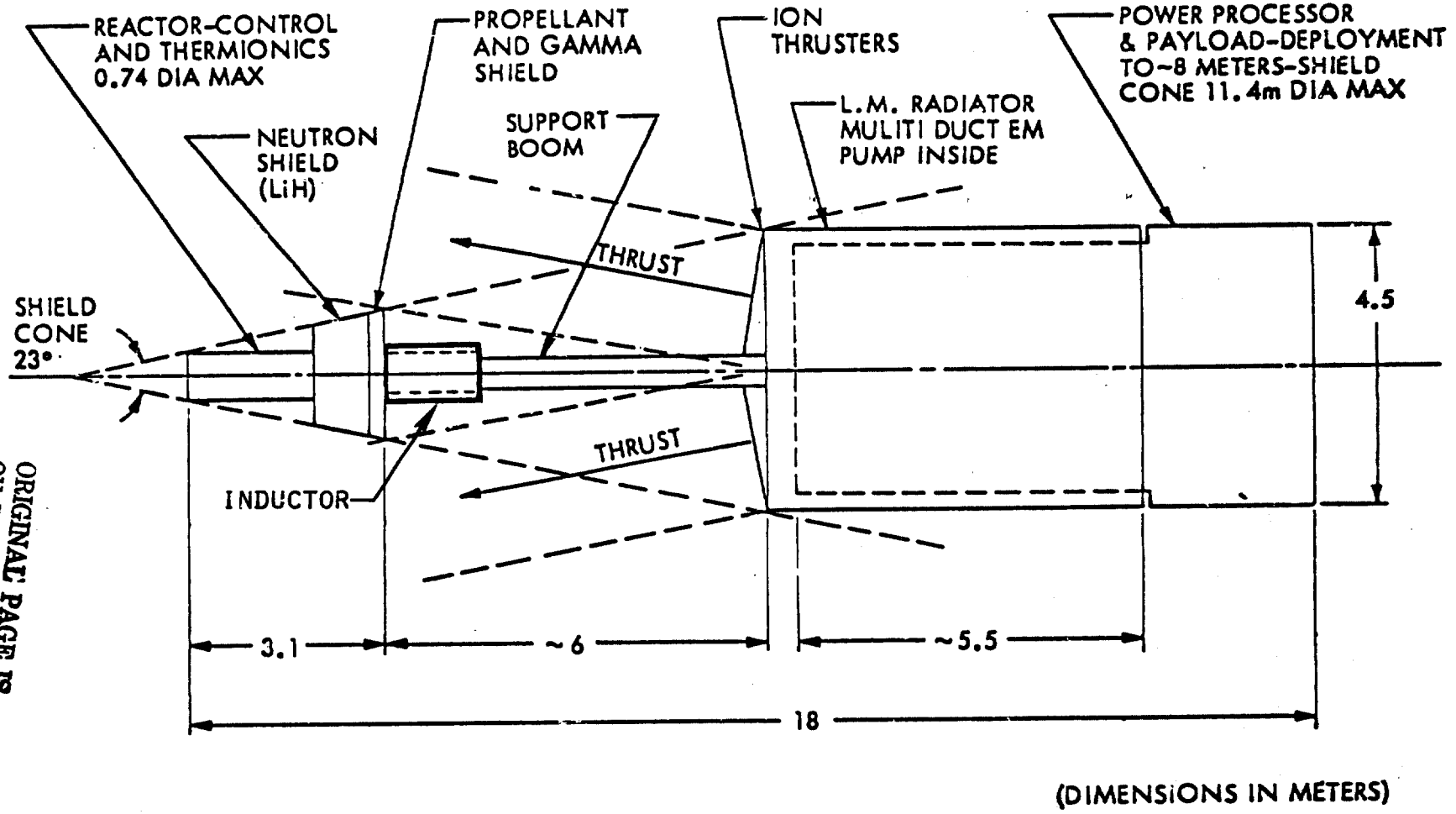

Fig. 1 Configuration of Shuttle Launched NEP Spacecraft

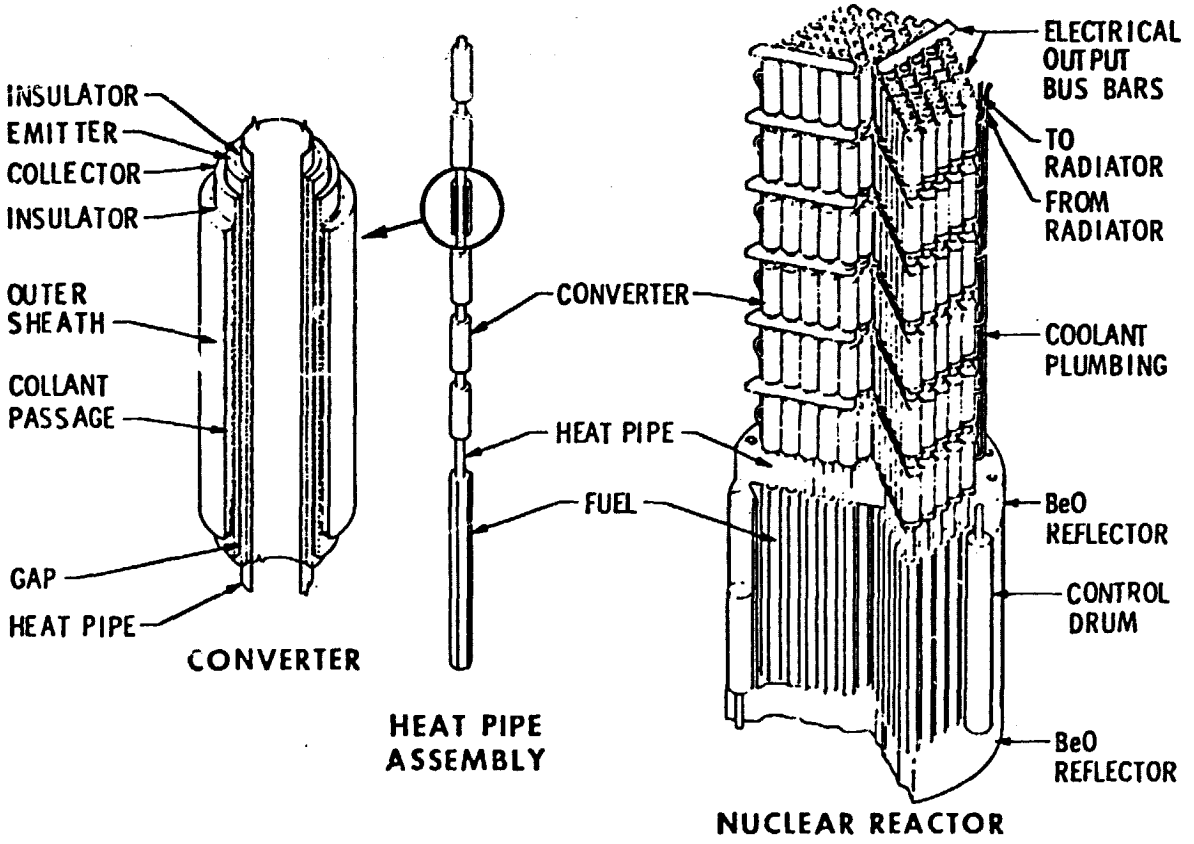

Fig. 2 JPL/LASL Out-of-Core Thermionic Reactor Design

The current voltage characteristic of a typical thermionic device is shown in Fig. 3a. For purposes of the analysis, a linear approximation was used for the current-voltage characteristic of the entire thermionic array as is shown in Fig. 3b. The open circuit voltage, shown on the figure as V_o, is 78 volts and the short circuit current, I_o, is 24,390 amps. The approximate I-V characteristic is written as

$$V_c = V_o(1 - I/I_o). \qquad (1)$$

The maximum power from the reactor, P_o occurs at approximately $V_o/2$ and $I_o/2$; i.e.

$$P_o = \frac{I_o V_o}{4} \qquad (2)$$

3.3 Magnetoplasmadynamic Thruster

Research on the quasi-steady MPD thruster is being carried out by the School of Engineering and Applied Sciences at Princeton University (Ref. 4). This Princeton program includes experiments to evaluate the thruster characteristics and demonstrate the use of inductive coupling. In this set of experiments, the power source is simulated by a capacitor bank.

The MPD thruster consists of a two electrode device and a propellant injection system as shown schematically in Fig. 4. The cylindrical cathode at the center is surrounded by an annular annode. Propellant is injected through the insulating back plate and accelerated out as a plasma to produce thrust. Current traveling axially down the cathode produces an azimuthal magnetic field. When the current then flows through the plasma it produces a $\vec{J} \times \vec{B}$ acceleration to move the plasma out the back of the thruster.

High currents are required by the thruster to produce the aximuthal self magnetic field. Operation of an MPD device at lower currents is possible but usually requires an externally generated magnetic field. The self field type operation is much preferred for better efficiency and lower mass.

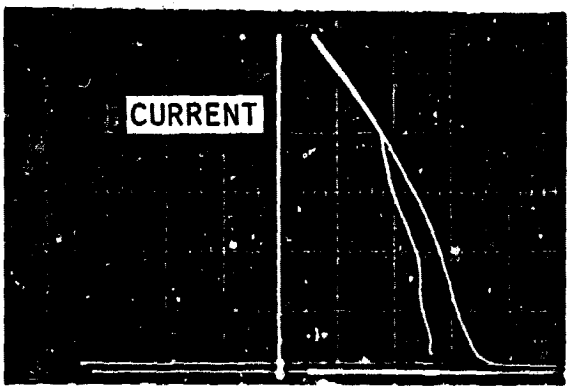

(a)

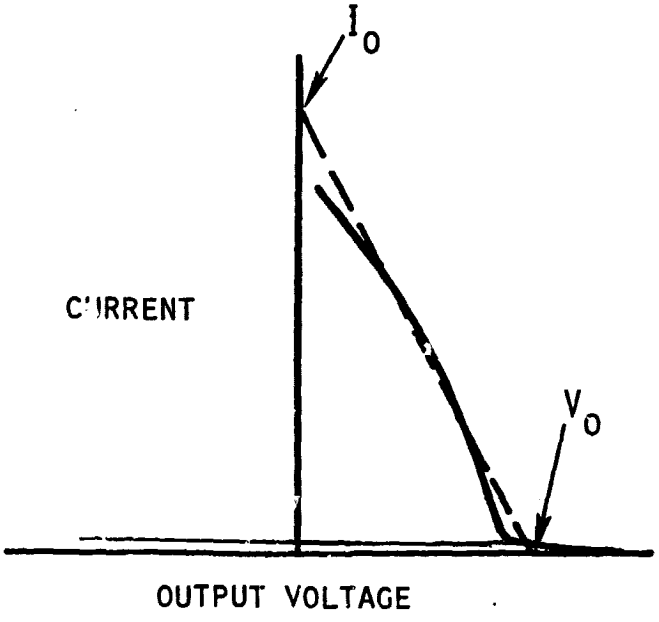

(b)

Fig. 3 Output Characteristics of Thermionic Power Sources (a) Typical I-V Curve of Cylindrical Thermionic Converter (b) Linear Approximation Representing the Output of a Thermionic Reactor. I_o = 24390 amps. V_o = 77.8 volts

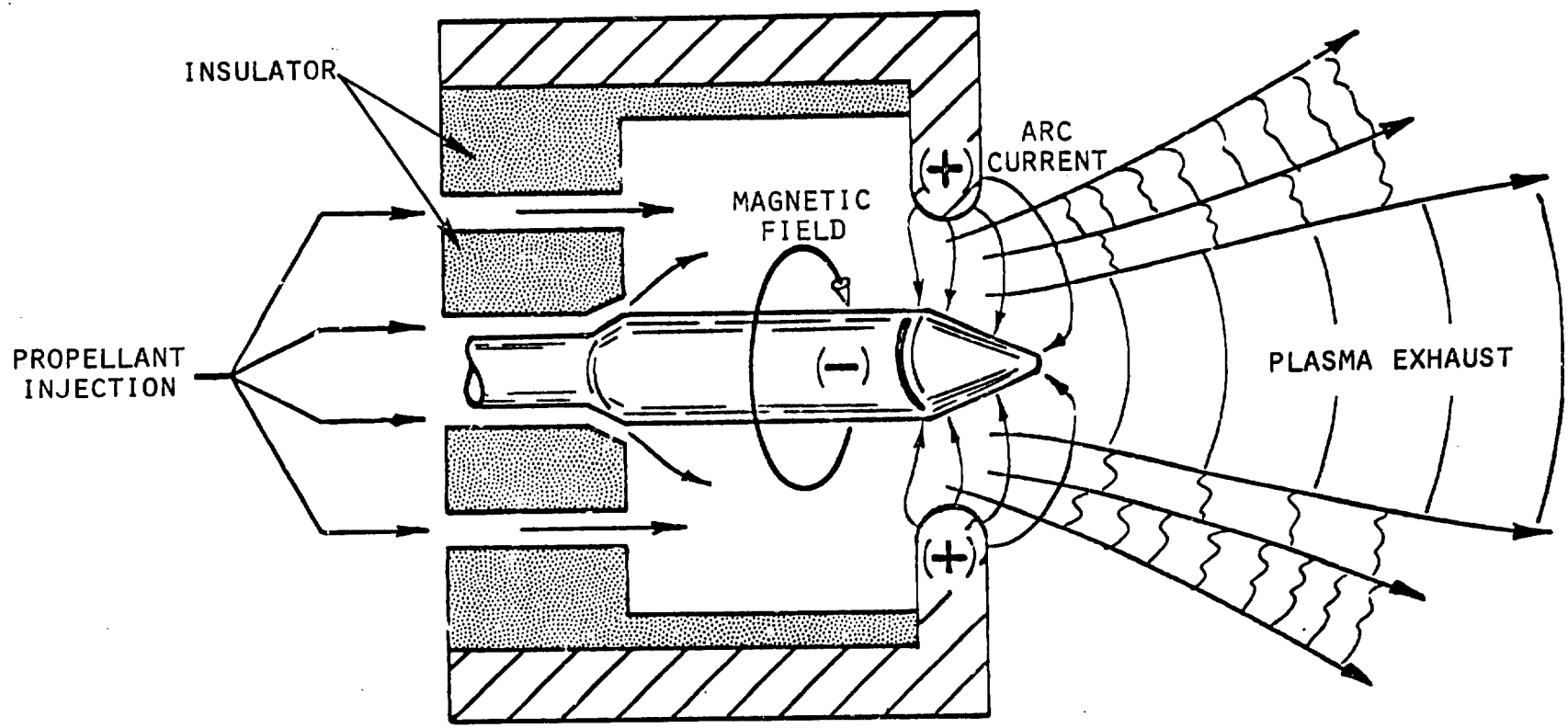

Fig. 4 Self-Field Magnetoplasmadynamic Accelerator (MPD Thruster)

The MPD thruster can use a variety of propellants since any medium through which an arc can be passed is capable of being accelerated. The propellant choice depends on the mission. Typical experimental MPD thrusters, currently being tested, use inert gases as propellants.

The voltage-current characteristic of an experimental MPD thruster previously tested at Princeton (Ref. 5) is shown in Fig. 5. As shown in the figure, there are two branches to the V-I characteristic. In the upper branch (high slope) the voltage is proportional to I^3. In order to model the V-I characteristic of the thruster for analytical purposes, the following equation was used.

$$V_T = V_F + \beta I^2 \qquad (3)$$

In Eq. (3) the thruster voltage is proportional to the 2nd power of the current. The form of Eq. (3) was selected even though a cubic approximation would be better because a cubic V-I characteristic leads to mathematical complexity in subsequent equations. The analytical approximation with $V_F = 30$ and $\beta = 1.2 \times 10^{-6}$ is compared with an experimental characteristic in Fig. 6.

4.0 INDUCTIVE COUPLING CIRCUITS

4.1 Transformer Type Circuit

To provide maximum flexibility in voltage transformation, it might be desirable to have an inductive unit with separate primary and secondary windings, i.e. a transformer. A schematic diagram which shows a transformer type circuit for coupling a thermionic reactor with a MPD thruster is presented in Fig. 7. By proper choice of the turns ratio between the primary and secondary, any desired voltage at the output can be obtained. The initial phase of this study centered around this type circuit.

Analysis shows that good coupling is possible at a variety of turns ratios. An important requirement for good efficiency is the speed of the control element S_1 (see Fig. 7). The control element must be capable of interrupting the primary current in a time significantly less than 1 msec. If S_1

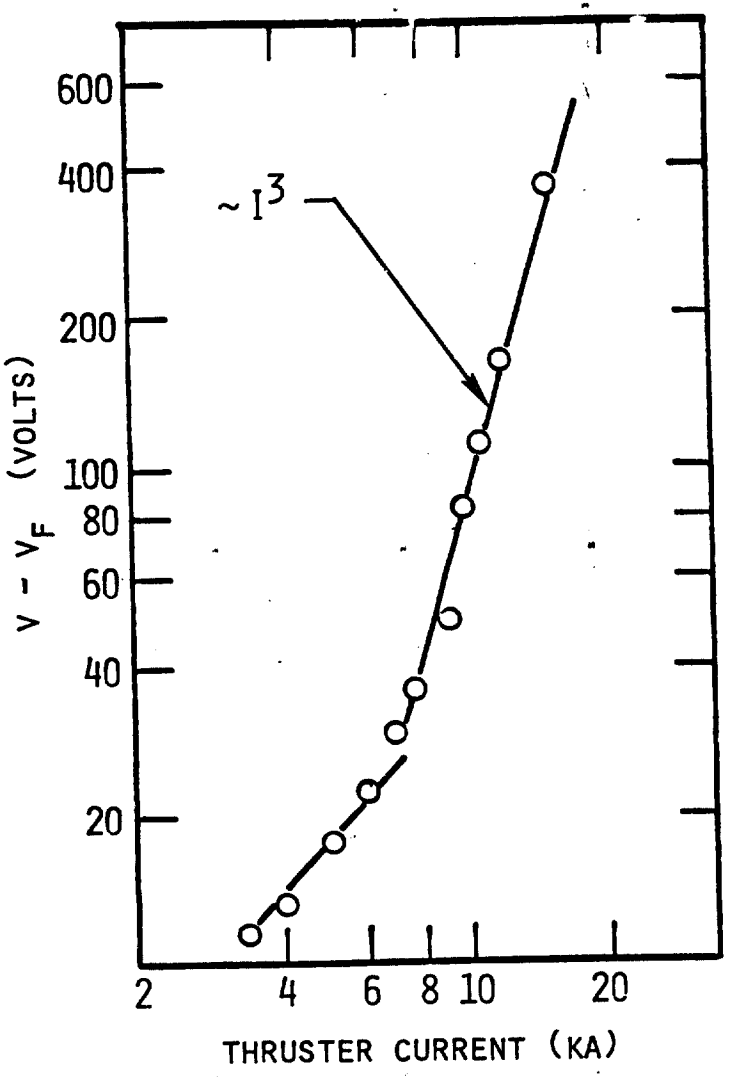

Fig. 5 Performance of an Experimental MPD Thruster at Princeton University. Propellant is argon. The I^3 dependence has a theoretical basis and does not depend on the electrode geometry.

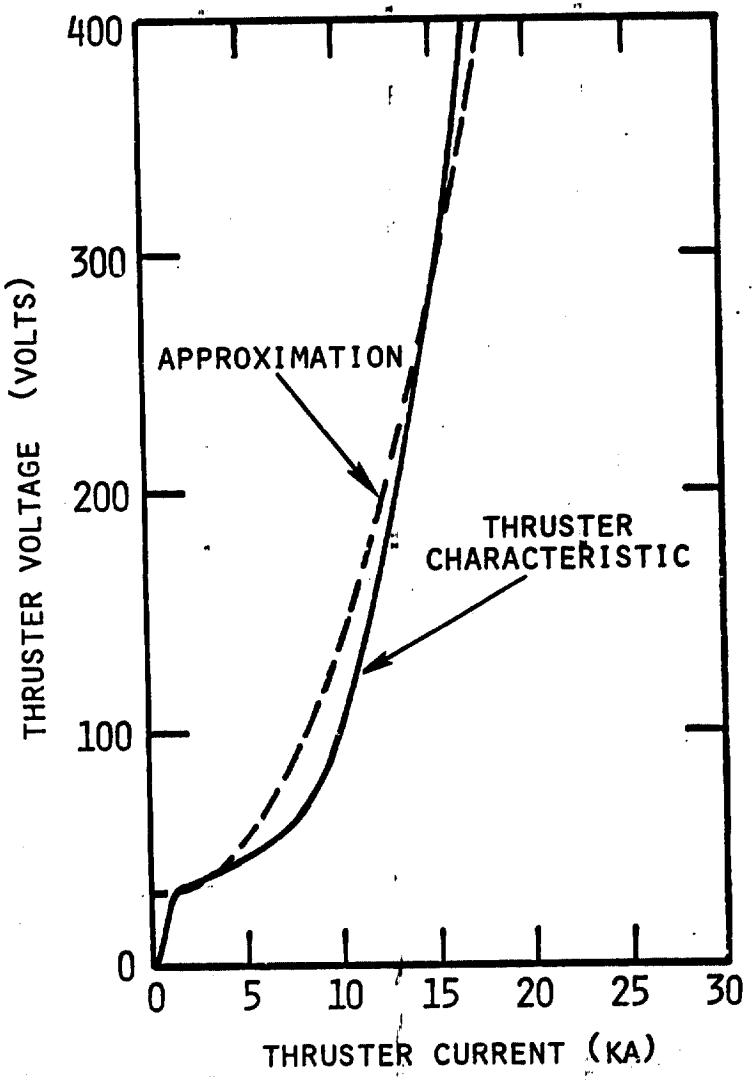

Fig, 6 Comparison of Analytical Approximation and Experimental MPD Thruster Characteristic. The approximate equation is $V_T = V_F + \beta I^2$, with $V_F = 30$ volts and $\beta = 1.2 \times 10^{-6}$ (amps)$^{-2}$.

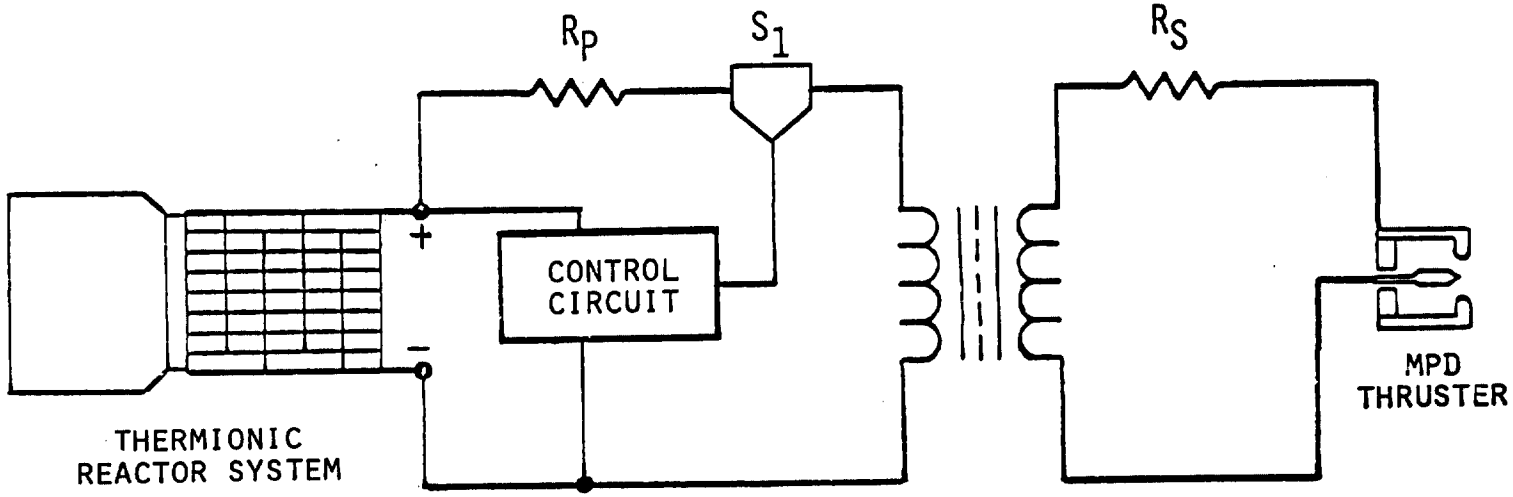

Fig. 7 Transformer Type of Circuit for Coupling Thermionic Reactor and MPD Thruster

does not reach a high impedance state ("open circuit") rapidly, large amounts of power are dissipated in the switch.

4.2 Self Inductor Circuit

One analytical result obtained with the transformer circuit is particularly interesting. This shows that a turns ratio of 1, i.e. a self inductor, is compatible with the nominal values stated earlier for the current and voltage in the thermionic converter array. A self inductor type of current is preferred because of the additional simplicity and lower mass available with a single winding. Consequently, greater emphasis has been placed on the self inductor circuit in the recent phase of this work.

A schematic of the self inductor circuit is shown in Fig. 8. As shown in the figure, the thruster is connected across the switching unit in this type of circuit. The switch is closed during the charging cycle and the current by-passes the thruster to build up a magnetic field in the inductor. During the thrust part of the cycle, the switch is open and the current is then forced to flow through the thruster unit. The current decays rapidly during this time consuming the energy which had been stored in the inductor during the charging cycle.

The particular device to be used as the switch in the circuit is not yet designed. However, an array of transistors or SCR's could be used for this purpose. For performance calculations it was assumed that a one volt drop occurs across the switch when it is in the closed position. A conceptual design for a switch of this type could consist of 100-200 semiconductors in parallel. Each semiconductor carries $\lesssim 100$ amps. Previous system analyses for spacecraft power conditioning have used transistors for inverter switching with similar operating characteristics (Ref. 6).

5.0 PERFORMANCE OF THE SELF-INDUCTOR CIRCUIT

5.1 Current Buildup

Using the linear approximation for the thermionic generating unit, a differential equation for the current buildup during the charging cycle can be written as follows:

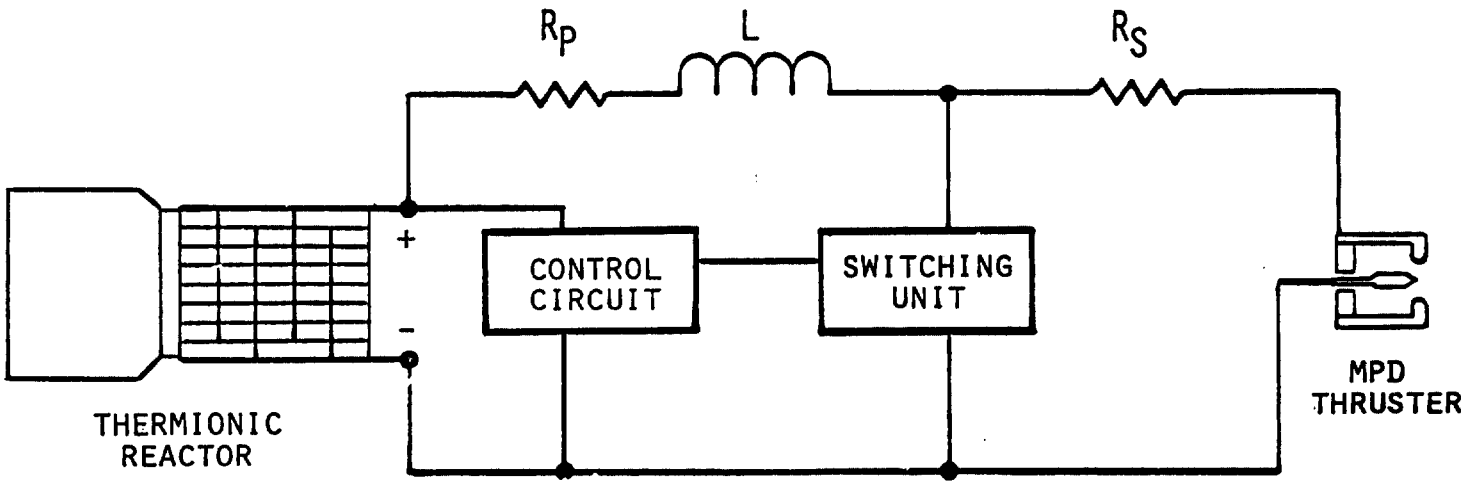

Fig. 8 Self Inductive Type of Circuit for Coupling a Thermionic Reactor and a MPD Thruster

$$L \frac{dI}{dt} + I R_p - V_o\left(1 - \frac{I}{I_o}\right) = 0 \qquad (4)$$

or

$$\frac{dI}{dt} + \frac{I}{\tau} - \frac{V_o}{L} = 0 \qquad (5)$$

where

$$\tau \equiv \frac{L}{R_p + V_o/I_o} \qquad (6)$$

Solving Eq. (5), and evaluating the constants using initial conditions yields the following result.

$$\hat{I} = \tilde{I} \exp\left(-\frac{T}{\tau}\right) + \left[\frac{V_o}{R_p + V_o/I_o}\right]\left[1 - \exp\left(-\frac{T}{\tau}\right)\right] \qquad (7)$$

5.2 Current During the Thrust Pulses

The thrust pulse begins when the switch is opened. The switch remains open during the thrust pulse. The turn-off time of the switch is assumed to be negligible ($\ll$ 1 msec). It may be possible to initiate the arc in the MPD thruster by the voltage transient as the switch opens. If this proves to be unfeasible, it is possible to use a small auxiliary pulse to start the arc in the MPD thruster. At the time the switch is opened, the current is at its maximum value. The decay of the current during the thrust pulse is described by the following differential equation.

$$L \frac{dI}{dt} + V_F + \beta I^2 - V_o\left(1 - \frac{I}{I_o}\right) = 0 \qquad (8)$$

During the thrust pulse the current falls to its final value $\tilde{I}$. Solution of Eq. (8) yields a relationship for $\tilde{I}$ as follows.

$$\tilde{I} \equiv I(t^*) = \left(\frac{\sqrt{q}}{2c}\right)\frac{1 + K \exp(-\sqrt{q}\, t^*)}{1 - K \exp(-\sqrt{q}\, t^*)} \tag{9}$$

where

$$K \equiv \frac{2c\,\hat{I} + b - \sqrt{q}}{2c\,\hat{I} + b + \sqrt{q}} \tag{10}$$

$$q \equiv b^2 - 4ac \tag{11}$$

$$a \equiv \frac{V_F - V_o}{L} \tag{12}$$

$$b \equiv \frac{R_p + R_s + V_o/I_o}{L} \tag{13}$$

$$c \equiv \frac{\beta}{L} \tag{14}$$

The values of $\hat{I}$, $\tilde{I}$, t^* and T as shown in Eqs. (7) and (9) are subject to optimization. It is desirable to have the current during the charging cycle remain as close as possible to the maximum power point of the thermionic converter array ($\sim$12000 amps). On the other hand effective use of the inductor requires that the difference between $\hat{I}$ and $\tilde{I}$ be as large as possible. It is also desirable to maintain the current through the thruster as high as possible. Because of these considerations, it is necessary to evaluate $\hat{I}$, $\tilde{I}$, t^* and T as part of the complete optimization.

6.0 CHARACTERISTICS OF THE INDUCTOR

6.1 Inductor Configuration

A system optimization requires detailed relationships for the variables which affect the characteristics of the inductor. A toroidal type of inductor may be preferred because it completely contains the magnetic field. Time-varying stray magnetic fields may be a source of interference for spacecraft instrumentation. However, it is difficult to design a toroidal inductor which will fit inside the shadow cone as shown in Fig. 1. As a result, a solenoidal inductor geometry was chosen for this study. A solenoid also has a better ratio of inductance to resistance than a toroid of equivalent mass. The size of the inductor shown in Fig. 1 is approximately to scale for a near optimum solenoidal configuration.

6.2 Inductance

The dimensions of the solenoidal inductor are shown in Fig. 9. All dimensions are in centimeters.

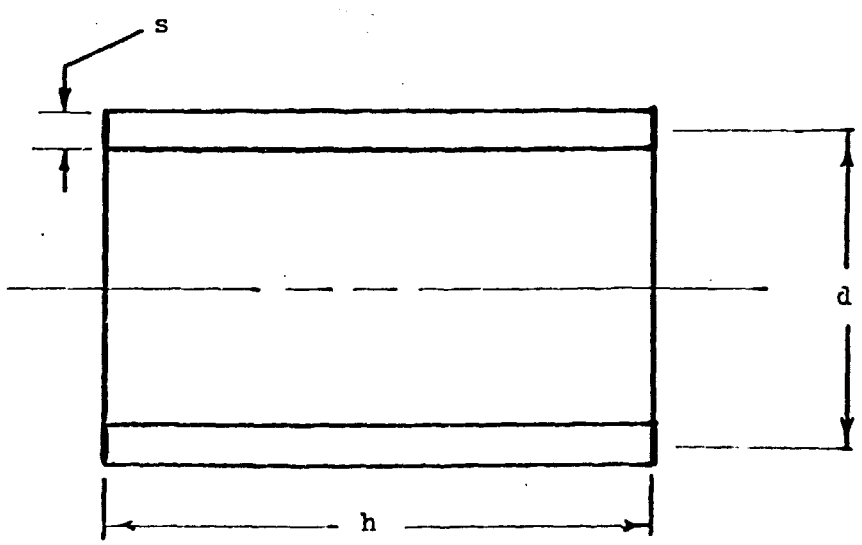

Fig. 9 Dimensions of Solenoid Inductor

The inductance of a solenoid of this type is given by Eq. (15) below:

$$L(\mu h) = \frac{N^2}{2.54}\left[Fd - \frac{.01596\ ds}{h}(.693 + B_s)\right] \qquad (15)$$

The functions F and B_s are tabulated in Ref. 7. However, the following analytical expressions have been obtained for these functions by curve fitting to the tabulated data.

$$F = .02378\ (d/h) - .00652\ (d/h)^2 \qquad (16)$$

$$B_s = .28 - .44\ \exp\left[-.45086\ (h/s)\right] \qquad (17)$$

6.3 Mass of the Inductor

The mass of the inductor varies inversely with the resistance of the winding. It's desirable to have the lowest possible resistance so it is necessary to compromise between the mass and the ohmic loss. The material which has the lowest ratio of mass density to electrical conductivity is aluminum (sodium has a lower value but it is not a practical choice). Consequently, the inductor windings are made of aluminum which is laminated to cut down eddy current losses. The laminations are assumed to take up 10% of the volume.

6.4 Resistance

The resistivity of aluminum is temperature dependent. Since significant ohmic losses will cause a temperature rise in the inductor it is necessary to use temperature dependent resistivity. An equation was fit to published data for the resistivity of aluminum (Ref. 8) as shown below.

$$\rho(\mu\Omega - cm) = 5.915 + .0232\ \theta - 1.75 \times 10^{-5}\ \theta^2 \qquad (18)$$

The value of the resistivity given by Eq. (18) is increased by 10% to account for the volume lost by lamination. This is then used to calculate the resistance of the helical inductance winding in the following equation

$$R = \frac{N\rho}{s}\left[\frac{(\pi d)^2 (N+1)^2}{h^2} + 1\right] \qquad (19)$$

6.5 Heat Balance

The thermal power generated by ohmic losses in the inductor is radiated from its outer surface. No additional radiator is necessary. The temperature of the inductor rises to approximately 600°K at thermal equilibrium by radiation. The above relationships for the characteristics of the inductor combined with previously derived equations for the performance of the thruster and the thermionic generating unit contain the necessary elements to perform a system optimization.

7.0 OPTIMIZATION

7.1 Coupling Effectiveness

Two criteria were used for optimization of the system. One is to maximize the coupling effectiveness, the other is to minimize the total specific mass of the power generating system and thrust unit.

The notion of coupling effectiveness requires some definition and discussion. The coupling effectiveness is defined as the average net power reaching the thruster divided by the maximum power available from the thermionic generating unit. This can be written as:

$$\eta \equiv \frac{P}{P_o} = \left(\frac{I}{\frac{1}{4} I_o V_o}\right)\left(\frac{\text{Energy Per Thrust Pulse}}{T + t^*}\right) \qquad (20)$$

This is not precisely the same as an efficiency. A major reason why η is not unity is that the current varies during a cycle and does not always

stay at the maximum power value, $I_o/2$. Only a portion of the power which is not coupled into the thruster is dissipated in ohmic and switching losses. For example, near the optimum approximately 14% of the maximum available power is not transferred to the thruster (η opt $\simeq$ 85%); but only approximately 6% is consumed by ohmic losses.

Thus, the value of η is a correct measure of the generating capacity required by the system, but it does not correctly determine reactor thermal power because the thermal input to the thermionic converters varies with current. The specific mass of the reactor is inversely proportional to the coupling effectiveness, but the specific mass of the radiator does not vary in the same way and neither does the fuel burn-up. Because of these facts, the estimates of specific mass for the entire system produced in this study are somewhat conservative.

7.2 Specific Mass

A previous study (Ref. 4) estimated the specific mass for the thermionic heat pipe reactor as α = 19.7 kg/KWe. This value was based on a system where the reactor gross power is 474 KWe and the net power is 400 KWe. It's convenient to redefine the specific mass value in terms of the gross power, thus

$$\alpha_R = 19.7\left(\frac{400}{474}\right) = 16.6 \text{ kg/KWe} \qquad (21)$$

This specific mass of the switching device is difficult to estimate since the switch is not defined. However for calculation purposes, the mass of transistors previously used for spacecraft power conditioning (Ref. 6) will be used. Each transistor caries 75 amperes; hence the number of transistors required is

$$\text{Number of Transistors} = \frac{I}{75} = \frac{2P_o}{75\ V_o} = \frac{2\ P}{75\ V_o \eta} \qquad (22)$$

The mass associated with the transistors and the appropriate connections is .35 kg per transistor (Ref. 6). Multiplying by the number of transistors given by Eq. (22) gives the specific mass of the switching device, α_T = .12 kg/KWe.

A small auxiliary radiator is required to dissipate the heat generated in the switching transistors. Specific mass of this radiator, α_{TR}, is estimated to be about 1 kg/KWe (Ref. 6).

The specific mass of a quasi-steady MPD thruster has been estimated as α_M = .6 kg/KWe in the power range of a few megawatts (Ref. 9). The total mass of the system can be written in terms of the net power and the coupling effectiveness as follows

$$\frac{\alpha_R P}{\eta} + \frac{\alpha_T P}{\eta} + \frac{\alpha_{TR} P}{\eta} + M_L + \alpha_M P = \text{Mass of System} \qquad (23)$$

Dividing through by the net power, P, yields the specific mass of the entire system

$$\alpha_S = \frac{\alpha_R + \alpha_T + \alpha_{TR}}{\eta} + \alpha_M + \frac{M_L}{P} \qquad (24)$$

or

$$\alpha_S = \frac{17.7}{\eta} + .6 + \frac{M_L}{400} \qquad (25)$$

Inspection of Eq. (25) shows that α_S varies inversely with the coupling effectiveness η and directly with the mass of the inductor M_L. The variation of the thruster efficiency is not directly included in the optimization. Hence, an arbitrary decision was made to keep the thruster current above 9,000 amperes for efficient operation. A nominal 1 msec duration was chosen for the thrust pulse which is near the optimum. Other variables were then optimized to yield a minimum in the system specific mass by an iterative calculation using

a HP 9820A programmable calculator. This calculator program and sample output are included as Appendices A and B respectively.

8.0 OPTIMIZATION RESULTS

The optimum value for the parameters of the inductive coupled system are as follows:

- Duration of the thrust pulse, $t^* = 1.0$ msec
- Time between pulses, $T = 4.5$ msec
- Maximum current $\hat{I} = 14.7$ kA
- Minimum current $\tilde{I} = 9.1$ kA
- Inductance, $L = 29$ μh (9 turns)
- Mass of the inductor $M_L = 950$ kg
- Coupling effectiveness $\eta = 86\%$
- System specific mass $\alpha_S = 23.5$ kg/KWe

Variations of the parameters in the vicinity of the optimum are shown in Fig. 10, 11, 12 and 13. The design point for the inductor mass (950 kg) is slightly higher than the value which yields a minimum in the specific mass. This value was selected to yield a higher coupling effectiveness and also to provide some safety factor in the design. The performance has a broad optimum with inductance in the range of 15-60 μh (7 to 13 turns) as shown in Fig. 11. The optimum value of the pulse duration is slightly above 1 msec as shown in Fig. 12. However, the 1 msec value was chosen as a design point to maintain a higher value of $\tilde{I}$ (refer to Eq. (9)). Similarly the optimum value of the time between pulses, T, is slightly less than 4.5 msec; however, the 4.5 msec value was retained as a design point to give the value of $\hat{I}$ (refer to Eq. (7)).

The waveforms of the current through the inductor and the power produced by the thruster are shown in Figs. 14(a) and (b). The duty cycle of the thruster is 22% at the design point.

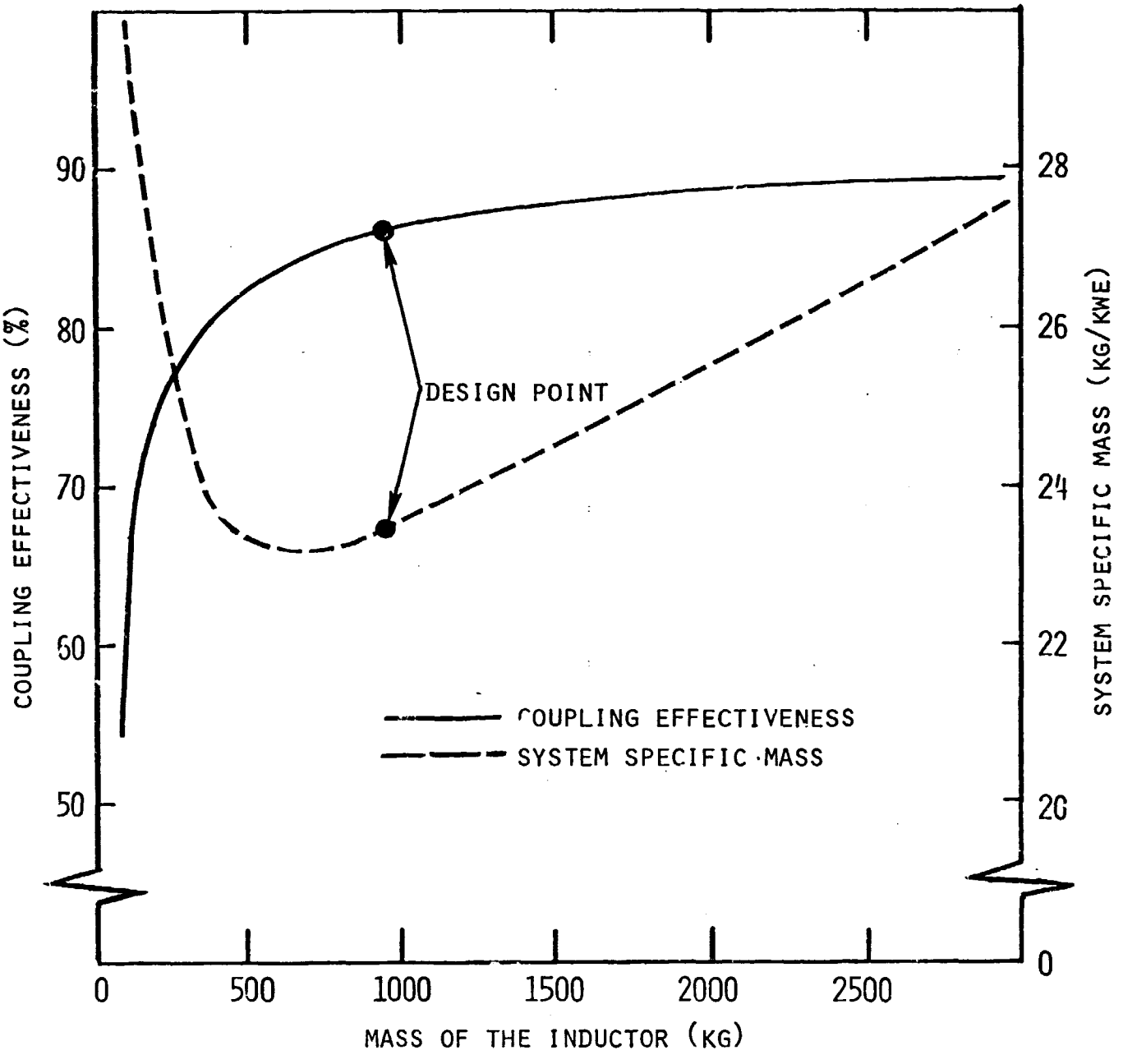

Fig. 10 Variation of Specific Mass and Coupling Effectiveness With Inductor Mass, M_L. Other parameters not varied in this figure: $t^* = 1.0$ msec; $T = 4.5$ msec; $L = 29$ μh.

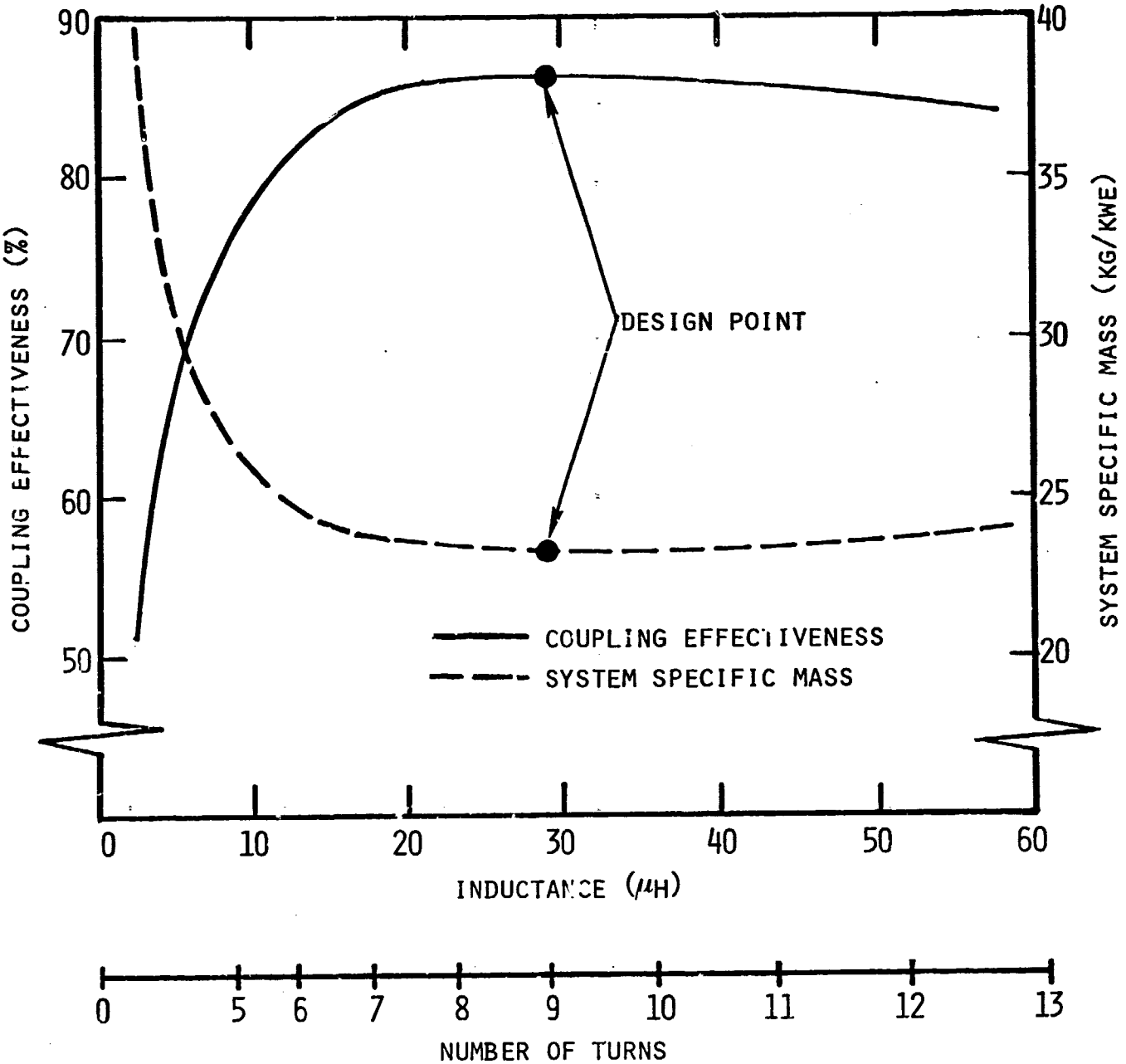

Fig. 11 Variation of Specific Mass and Coupling Effectiveness With Inductances, L. Other parameters not varied in this figure: $t^* = 1.0$ msec; $T = 4.5$ msec; $M_L = 950$ kg.

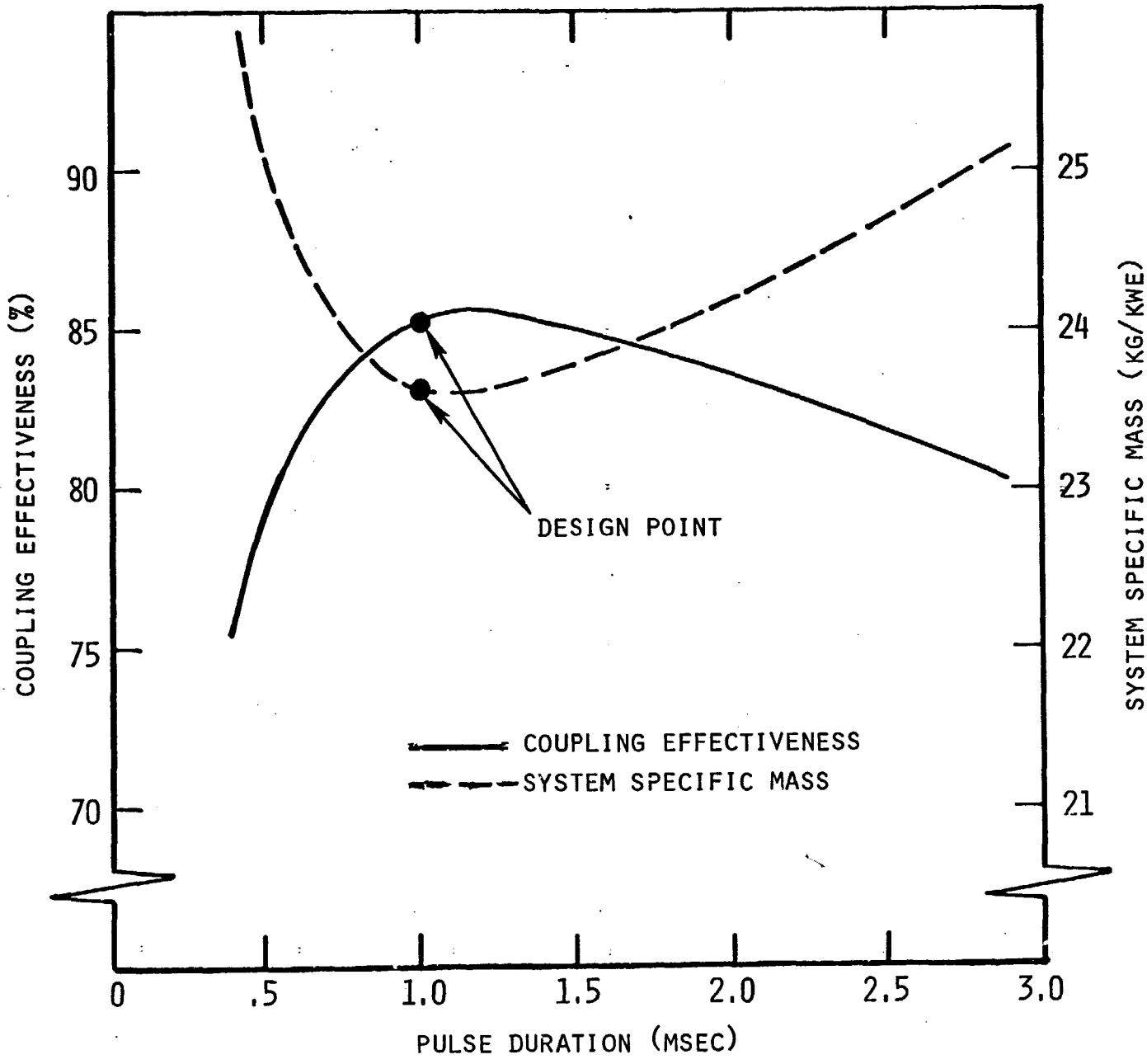

Fig. 12 Variation of Specific Mass and Coupling Effectiveness With Pulse Duration, t*. Other parameters not varied in this figure: T = 4.5 msec; L = 29 μh; M_L = 950 kg.

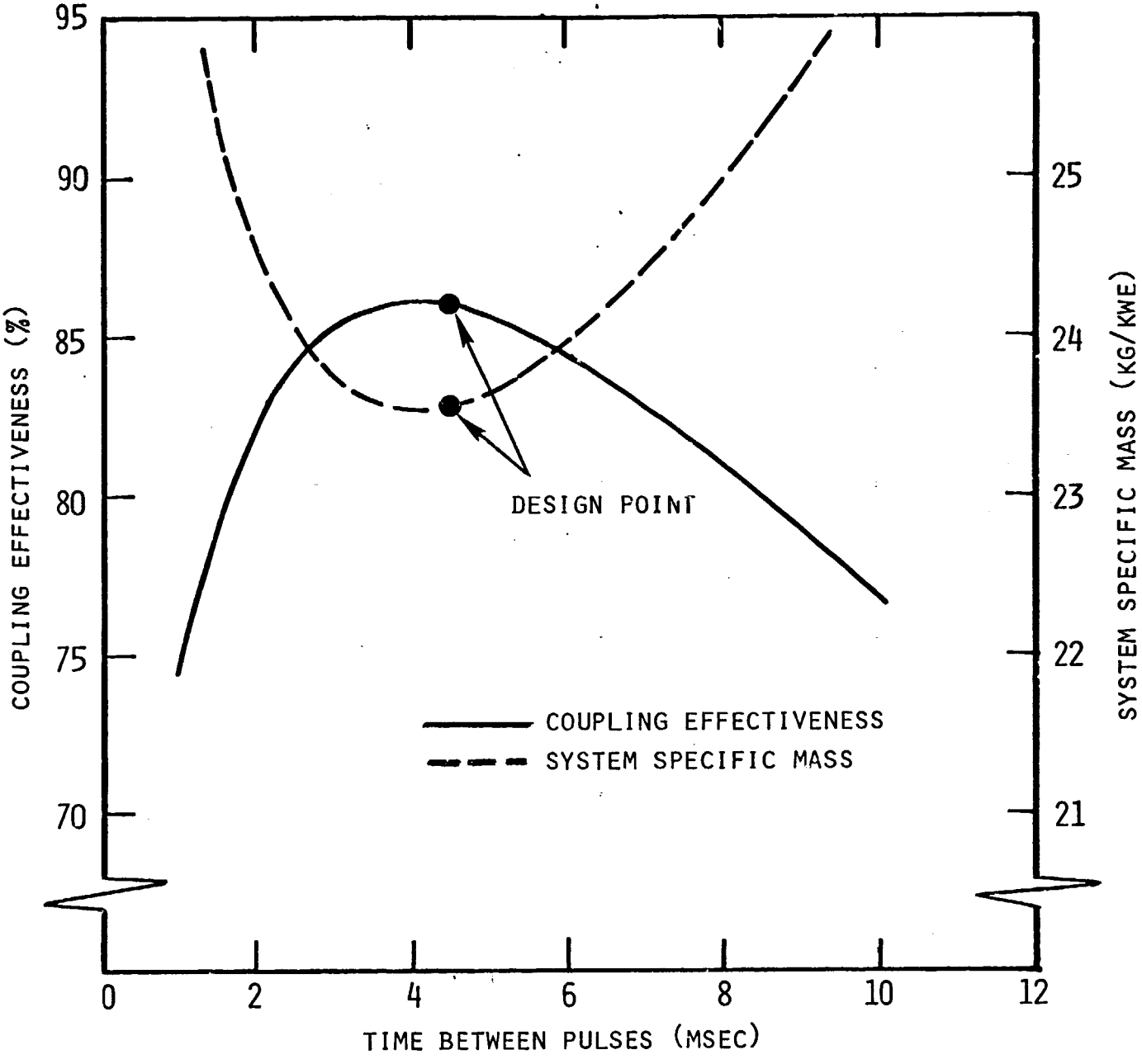

Fig. 13 Variation Specific Mass and Coupling Effectiveness With Time Between Pulses, T. Other parameters not varied in this figure: $t^* = 1.0$ msec; L = 29 μh, M_L = 950 kg.

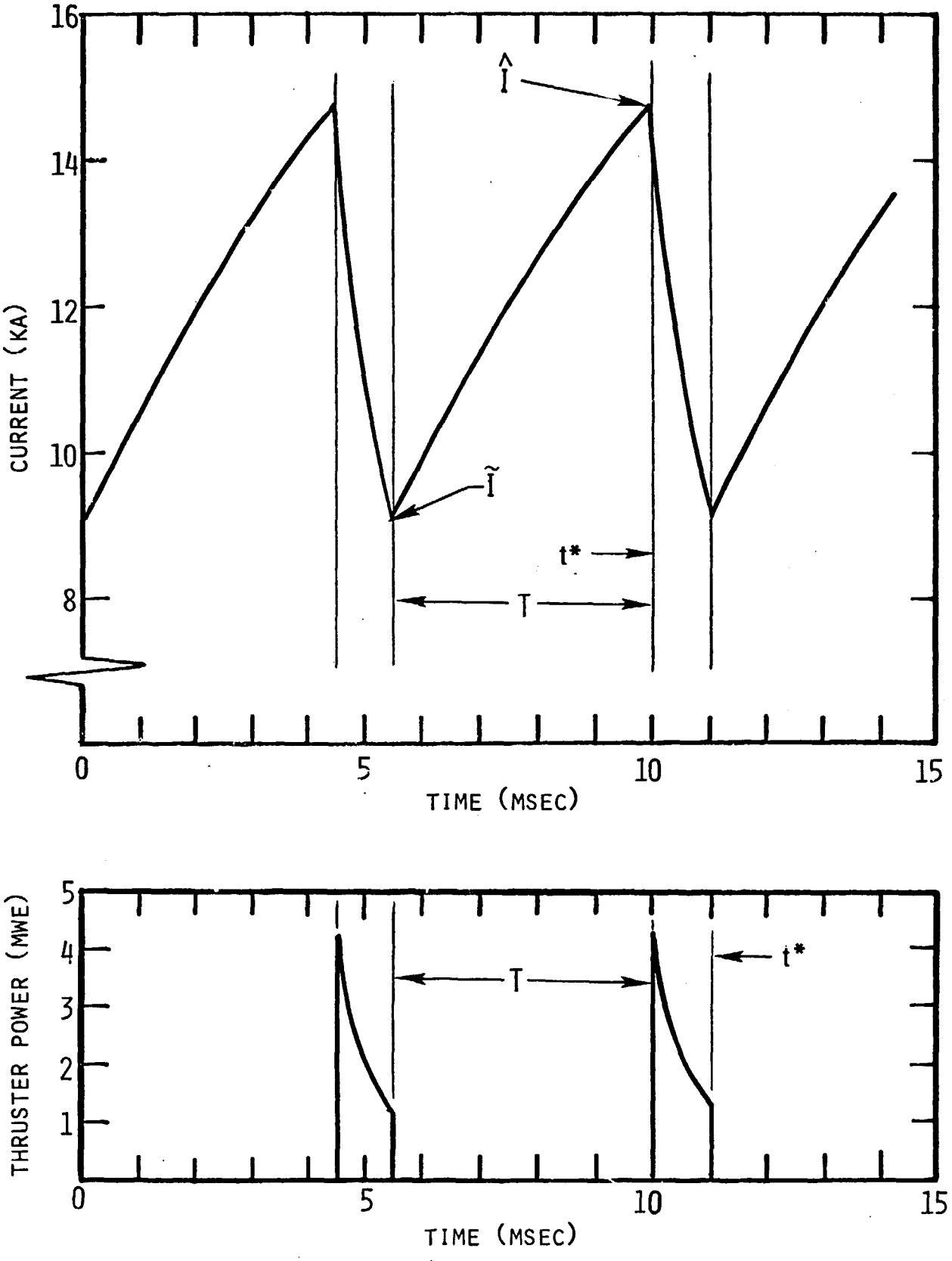

Fig. 14 Waveforms of Inductor Current and MPD Thruster Power at Optimized Design Point. $\hat{I}$ = 14.7 kA; $\tilde{I}$ = 9.1 kA; T = 4,5 msec; t* = 1.0 msec.

9.0 SUMMARY AND CONCLUSIONS

The results of the preliminary analysis have shown that an inductively coupled thermionic reactor and an MPD thruster is a potentially attractive system for spacecraft electric propulsion. Good coupling efficiency has been shown to be possible. Specific mass of a nuclear electric propulsion system using ion rockets is calculated to be ~ 28 kg/KWe (Ref. 3). Thus the specific mass estimate of 23.5 kg/KWe for the TI-MPD system obtained in this work appears to be competitive.

Additional experimental and analytical work must be accomplished before the system is proven flight ready. Experimental data are needed to assess the performance of an MPD thruster when driven by an inductive source. An important remaining design uncertainty is the current interrupting switch (solid state or other). Design of a switching circuit to interrupt large currents in an inductive circuit is somewhat difficult.

If the remaining considerations can be satisfactorily treated by continued development, the thermionic - MPD system will be an important option for future space missions.

10.0 REFERENCES

1. Estabrook, W.C., et.al., "Comparative Assessment of Out-of-Core Nuclear Thermionic Power Systems", Technical Memorandum 33-749 Jet Propulsion Laboratory, Nov. 15, 1975.

2. "JPL/LASL Heat Pipe/Thermionic Reactor Technology Development Program", Quarterly Progress Report, Jet Propulsion Laboratory, Oct. 15, 1975.

3. "JPL/LASL Heat Pipe Thermionic Reactor Technology Development Program", Quarterly Progress Report, Jet Propulsion Laboratory, Jan. 15, 1976

4. "Pulsed Electromagnetic Gas Acceleration", Semi-Annual Report 634y, Department of Aerospace and Mechanical Sciences, Princeton University, July 1975.

5. Boyle, M.J. et.al., "Flow Field Characteristics and Performance Limitations of Quasi-Steady Magnetoplasmadynamic Accelerators", AIAA 11th Electric Propulsion Conference, AIAA Paper No. 75-414, New Orleans, 1975.

6. Gietzen, A.J., "Low Voltage Power Conditioning For a Thermionic Reactor", Progress Report GAMD-9603, Gulf General Atomic Inc., July 16, 1969.

7. Terman, F.E. Radio Engineers Handbook, McGraw-Hill, N.Y., 1943, pp 53-61.

8. Handbook of Chemistry and Physics, 41st Edition, Chemical Rubber Publishing Co., Cleveland, Ohio, 1960, p 2589.

9. Jahn, R.G. and Clark, K.E., "Energy Management Technology Forecast For Space Operations and Propulsion: Electromagnetic Accelerator", Princeton University, Princeton, New Jersey, Jan. 2, 1975.

APPENDIX A

A COMPUTER PROGRAM FOR CALCULATING THE PERFORMANCE OF THE TI-MPD SYSTEM

```
46:
PRT "PRIMARY STO
RED","ENERGY (J)
",.5E-6R2(R32↑2-
YY)→R16⊢
47:
PRT "MPD PULSE P
OWER","MEGAWATTS
",.001R15/R1⊢
48:
PRT "MPD AVG POW
ER","KILOWATTS",
R15/(R1+R6)→R17⊢
49:
PRT "THERMIONIC"
,"MAX POWER (KWE
)",R19(R4+1)↑2/4
000R4→R28⊢
50:
PRT "TRANSFER","
EFFICIENCY (%)",
100R17/R28→R18;
SPC 5⊢
51:
PRT "OHMIC LOSS
(KW)",.001R30R30
*1E-6R3→R50⊢
52:
PRT "HEAT RAD. (
KW)",5.67E-15R47
R46↑4→R51⊢
53:
IF R50<R51;GTO "
↑"⊢
54:
SPC 2;PRT "***NO
T SELF*****","**
*RADIATING****";
SPC 2⊢
55:
"↑";PRT "IND (KG
/KWE)",R49/R17→R
52⊢
56:
PRT "SYST (KG/KW
E)",R52+.6+1774/
R18→R53⊢
57:
PRT "***********
*******";SPC 8⊢
58:
END ⊢
R58
```

```
0:
"RP";-5.8150075+
.032305P5-1.75E-
5P5P5→P6;1.1P6→P
6⊢
1:
IF P4>1;GTO +2⊢
2:
πP1P6/P2P3→P7;
GTO "VAL"⊢
3:
(πP1)↑2*(P4+1)↑2
/P2P2+1→P8;P4P6r
P8/P3→P7⊢
4:
"VAL";P7→F ⊢
5:
END ⊢
R58
```

```
0:
"L(UH) ";P1/P2→P
8;P2/P3→P9;.0237
8P8-.00652P8P8→P
5⊢
1:
.28-.44EXP (-.45
086P9)→P6⊢
2:
P5P1-.01596(.693
+P6)/P2→P10;P4P4
P10/2.54→F ⊢
3:
END ⊢
R58
```

```
0:
"I MIN";EXP (-R0
P1)→P3;(2CP2+B-R
0)/(2CP2+B+R0)→P
4⊢
1:
1+P4P3→P5;1-P4P3
→P6⊢
2:
(R0/2C)(P5/P6)-B
/2C→F ⊢
3:
END ⊢
R58
```

```
0:
"I MAX";EXP (-P1
R33/1E-6R2)→P3;P
2P3+(R4/R33)(1-P
3)→F ⊢
1:
END ⊢
R58
```

```
0:
CFG 3;CFG 1⊢
1:
ENT "INDCT. OD (
CM)",R41,"THICKN
ESS (CM)",R44,"L
ENGTH (CM)",R43⊢
2:
PRT "INDCT. OD (
CM)",R41,"THICKN
ESS (CM)",R44,"L
ENGTH (CM)",R43⊢
3:
ENT "NO. OF TURN
S",R45,"TEMP. (D
EG K)",R46⊢
4:
PRT "NO. OF TURN
S",R45,"TEMP. (D
EG K)",R46⊢
5:
R41-R44→R42;πR41
R43→R47;R41↑2-(R
41-2R44)↑2→Z⊢
6:
πR43Z/4→R48;.002
7R48→R49⊢
7:
RP(R42,R43,R44,R
45,R46)→R3;
L(UH) (R42,R43,R
44,R45)→R2⊢
8:
SPC 2;PRT "AREA
(CM2)",R47,"MASS
 (KG)",R49⊢
9:
PRT "RP (UOHMS)"
,R3,"L (UH)",R2;
SPC 8;STP ⊢
10:
ENT "DELTA T* (M
SEC)",R1⊢
11:
PRT "DELTA T* (M
SEC)",R1⊢
12:
ENT "RS (MILLIOH
MS)",R5,"T (MSEC
)",R6,"BETA (KA↑
2)",R7⊢
13:
PRT "RS (MILLIOH
MS)",R5,"T (MSEC
)",R6,"BETA (KA↑
2)",R7⊢
14:
ENT "V0 (VOLTS)"
,R4,"I0 (AMPS)",
R19⊢
15:
PRT "V0 (VOLTS)"
,R4,"I0 (AMPS)",
R19;SPC 3⊢
16:
ENT "NO. OF INT
STEPS",R37;PRT "
NO. OF INT STEPS
",R37⊢
17:
ENT "NO. OF PRIN
TS",R35;PRT "NO:
 OF PRINTS",R35;
SPC 5⊢
18:
(30-R4)/1E-6R2→A
;(1E-6R3+.001R5+
R4/R19)/1E-6R2→B
;R7/R2→C⊢
19:
R4/R19+1E-6R3→R3
3⊢
20:
0→X→R15→R22→R25→
R14;√(BB-4AC)→R0
⊢
21:
R19/4→R29;R19→R3
1⊢
22:
"INT";I MAX(.001
R6,R29)→R30;ABS
(R30-R31)/R30→R3
4⊢
23:
IF R34≤.0001;R30
→R32;GTO "CON"⊢
24:
R30→R31;I MIN(.0
01R1,R30)→R29⊢
25:
GTO "INT"⊢
26:
"CON";(2CR32+B-R
0)/(2CR32+B+R0)→
R12;SFC 1⊢
27:
IF R35=0;0→R26;
GTO +2⊢
28:
R1/R35→R26⊢
29:
IF R37=0;0→R27;
GTO +2⊢
30:
R26/R37→R27⊢
31:
"LOOP";XR26→R38;
0→R36⊢
32:
"LEEP";R38+R36R2
7→R11⊢
33:
EXP (-.001R0R11)
→R8;1+R12R8→R9;1
-R12R8→R10⊢
34:
(R0/2C)(R9/R10)-
B/2C→Y⊢
35:
1E-6R7*YY+30→R13
;YR13→R21⊢
36:
IF FLG 1;GTO "PR
NT"⊢
37:
(R21+R22)/2→R23;
.001(R11-R14)R23
→R24;R24+R25→R15
⊢
38:
R21→R22;R15→R25;
R11→R14⊢
39:
R36+1→R36;IF R36
≤R37;GTO "LEEP"⊢
40:
"PRNT";PRT "T (M
SEC)",R11,"I(T)"
,Y⊢
41:
PRT "MPD VOLTAGE
",R13⊢
42:
PRT "MPD POWER (
MWE)",R21/1E6⊢
43:
PRT "MPD ENERGY
(J)",R15;SPC 4⊢
44:
IF FLG 1;CFG 1;
GTO "LOOP"⊢
45:
X+1→X;IF R1>R11;
GTO "LOOP"⊢
```

APPENDIX B

TYPICAL COMPUTER OUTPUT - NEAR OPTIMUM CONDITIONS

INDCT. OD (CM)
90.000
THICKNESS (CM)
10.000
LENGTH (CM)
140.000
NO. OF TURNS
9.000
TEMP. (DEG K)
600.000

AREA (CM2)
39584.067
MASS (KG)
950.018
RP (UOHMS)
129.370
L (UH)
29.232

DELTA T* (MSEC)
1.000
RS (MILLIOHMS)
1.000
T (MSEC)
4.500
BETA (KA↑2)
1.200
V0 (VOLTS)
76.760
I0 (AMPS)
24076.343

NO. OF INT STEPS
50.000
NO. OF PRINTS
1.000

T (MSEC)
0.000
I(T)
14754.015
MPD VOLTAGE
291.217
MPD POWER (MWE)
4.297
MPD ENERGY (J)
0.000

T (MSEC)
1.000
I(T)
9166.851
MPD VOLTAGE
130.837
MPD POWER (MWE)
1.199
MPD ENERGY (J)
2255.438

PRIMARY STORED
ENERGY (J)
1953.423
MPD PULSE POWER
MEGAWATTS
2.255
MPD AVG POWER
KILOWATTS
410.080
THERMIONIC
MAX POWER (KWE)
474.142
TRANSFER
EFFICIENCY (%)
86.489

OHMIC LOSS (KW)
28.161
HEAT RAD. (KW)
29.088
IND.(KG/KWE)
2.317
SYST (KG/KWE)
23.428